The Equation of State for a one-component System

H. P. Neumann

Institut für Physikalische Chemie der Universität Frankfurt/Main

(Z. Naturforsch. **29 a**, 65–74 [1974]; received 5 Oct. 1971, in final form 13 August 1973)

The Equation of State for a one-component System

The cooperative problem for a lattice gas on a plane, square lattice and on a simple cubic lattice is solved by a system of two coupled, transcendental equations, derived by a combinatorial method, which describes a homogeneous or periodical particle density on the lattice as a function of the temperature and the chemical potential of the lattice-gas.

For the particle interaction a Hard-Core potential (nearest neighbour exclusion) with a soft long-range tail is assumed. The zero-component of the Fourier-transform of this long-range interaction part can be positive or negative.

The system of transcendental equations is solved by a graphic method.

As a result, the complete pressure-density state diagram and the pressure-temperature phase diagram can be drawn.

The lattice-gas exists in three stable phases: gas, liquid and solid. Three phase changes are possible: condensation, crystallization and sublimation.

Critical points of condensation and freezing are examined. The number of possible phases and phase changes at a fixed temperature depends on the geometric structure of the particle interaction.

1. Introduction

Among many attempts, to derive an equation of state for liquids and gases by methods of statistical mechanics, the replacement of the configurational part of the partition function of a real system by that of an Ising lattice gas model was very successful[1–15].

On the other hand the extension of this theory of the equation of state to solid phases, including liquid-solid and gas-solid phase transitions however, is a very difficult task in general[16–34].

Similar difficulties arise in the case of some generalized Ising models for magnetic systems[35–40] which are able to describe several phase transitions.

In this article a model describing several phases and phase transitions is proposed. The main result is an equation of state of a lattice system which predicts the existence of the three phases: gas, liquid, and solid together with the three phase transitions: condensation, crystallization, and sublimation.

Starting from the classical mechanical properties, the interaction part of the hamiltonian H_{LG} for the lattice model may be written in the form

$$H_{LG} = -\tfrac{1}{2} \sum_{i,j=1}^{V} v_{ij}(\varepsilon_i, \varepsilon_j)\,. \tag{1}$$

The interaction $-v_{ij}(\varepsilon_i, \varepsilon_j)$ fulfills the following conditions:

1) $v_{ij} = 0$ for $i = j$.
2) If i, j are nearest neighbour lattice sites v_{ij} is of the form
   $v_{ij}(1{,}1) = -\infty$, $v_{ij}(1{,}0) = v_{ij}(0{,}1) = v_{ij}(0{,}0) = 0$.
3) For all other pairs i, j the interaction is "Ising like" $v_{ij}(\varepsilon_i, \varepsilon_j) = v_{ij}\, \varepsilon_i\, \varepsilon_j$ with $\sum_{j=1}^{V}{}'' \, v_{ij} < \infty$, where the sum extends over all pairs $(i \neq j)$ which are *not* nearest neighbours.

ε_i and ε_j are particle occupation numbers at the sites i and j which assume the values 1 (occupied by one particle) or 0 (empty). V is the total number of lattice sites.

Using this hamiltonian the equation of state can be calculated by the grand partition function[3]:

$$\Xi = \sum_{\varepsilon_1=0}^{1} \sum_{\varepsilon_2=0}^{1} \cdots \sum_{\varepsilon_V=0}^{1} \times \exp\left[\beta\left(\frac{1}{2} \sum_{i,j=1}^{V} v_{ij}(\varepsilon_i, \varepsilon_j) + \mu \sum_{i=1}^{V} \varepsilon_i\right)\right]. \tag{2}$$

($\beta = 1/kT$, T = absolute temperature, μ = chemical potential, containing the kinetic part of the hamiltonian).

Inserting (2) into

$$p\,V = \frac{1}{\beta} \ln \Xi = -(E - TS - \mu N) \tag{3}$$

Sonderdruckanforderungen an Dr. H. P. Neumann, Dozent am Institut für Physikalische Chemie der Universität Frankfurt/M., *D-6000 Frankfurt (Main)*, Robert-Mayer-Str. 11.

the equation of state for the lattice model results. (p = pressure, V = volume, N = total number of particles, E = interaction part of the internal energy, S = entropy. — Having $\bar{V}$ sites on the total lattice, in the configuration of highest density on the plane square and the simple cubic lattice $\bar{V}/2$ lattice sites are occupied, for example the black sites in Figure 1. The maximal density is then $\bar{V}/2\,V = \varrho_{\mathrm{HC}} = 1/v_{\mathrm{HC}}$, where v_{HC} is the hard core volume. Measuring the volume in suitable units one can set $V = \bar{V}$).

In thermodynamic equilibrium we expect two structures to occur:

an inhomogeneous "periodical" structure, for which the densities ϱ_i on two sublattices ($i = 1, 2$) are different ("crystalline" or "solid" structure), and a homogeneous one, for which $\varrho_1 = \varrho_2$ ("fluid" structure).

The densities ϱ_1 and ϱ_2 are, apart from the dimension, identical with the mean occupation numbers $\langle\varepsilon\rangle(1) = N_1/\frac{1}{2}V$ and $\langle\varepsilon\rangle(2) = N_2/\frac{1}{2}V$ on the two sublattices.

How to derive this assumption from the partition function Ξ is an interesting, but open question. For the crystalline phase on the plane square lattice, the periodic structure shown in Fig. 1, will be considered only. An equivalent periodic structure will be regarded for the simple cubic lattice.

Given the two unequal densities ϱ_1 and ϱ_2 of the periodic distribution, the grand canonical partition function in (2) may be written

$$\Xi = \sum_{\varrho_1}\sum_{\varrho_2} W(\varrho_1, \varrho_2)\left\{\left[\sum_{\substack{\varepsilon_1,\ldots,\varepsilon_V \\ \Sigma\varepsilon_i(1) = N_1 = \varrho_1 V/2 \\ \Sigma\varepsilon_i(2) = N_2 = \varrho_2 V/2}}{}' \exp\left[\beta\,\tfrac{1}{2}\sum_{i,j=1}^{V} v_{ij}(\varepsilon_i, \varepsilon_j) + \beta\,\mu\sum_{i=1}^{V}\varepsilon_i\right]\right] \Big/ W(\varrho_1, \varrho_2)\right\}, \tag{4}$$

where $\sum'_{\varepsilon_1,\ldots,\varepsilon_V}$ is the restricted sum over states with fixed particle densities ϱ_1, ϱ_2 on the sublattices 1 and 2 and $W(\varrho_1, \varrho_2)$ gives the number of nonvanishing terms with ϱ_1 = constant and ϱ_2 = constant, which are in concord with the nearest neighbour hard core interaction. The sums $\sum_{\varrho_1}$ and $\sum_{\varrho_2}$ extend over all possible values of ϱ_1 and ϱ_2 with $0 \leqq \varrho_1 \leqq 1$ and $0 \leqq \varrho_2 \leqq 1$, which must be, of course, also in concord with the hard core interaction. The sums become integrals in the thermodynamic limit N, $V \to \infty$.

On the other hand it follows from the equations for ϱ_i that for the fluid case, where the particle distribution on the lattice is homogeneous and may be characterized by an ensemble average $\langle\varepsilon\rangle = \varrho$ independent of the lattice site index i, two different phases can occur: a high density phase ("liquid") and a low density phase ("gas") for certain ranges of T, μ. In the case of several different solutions, the thermodynamically most stable ones are chosen.

Also transitions between these three phases (solid or crystalline, liquid and gas phase) are possible. These are: Crystallization and melting, evaporation and condensation or sublimation.

2. Development of General Equations for the Thermodynamic State-Variables of the Lattice Model

The combinatorial derivation of $W(\varrho_1, \varrho_2)$ from (4) may be presented in the case of the plane square lattice. The derivation for the linear lattice and the simple cubic lattice is quite the same.

In Fig. 1 it is shown how the plane, square lattice is divided into two similar plane, square sublattices.

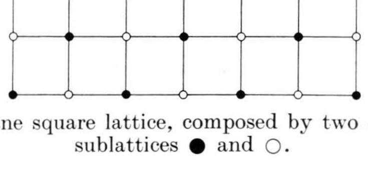

Fig. 1. Plane square lattice, composed by two equivalent sublattices ● and ○.

As a convention the black sites in Fig. 1 may be statistically more occupied with particles than the white sites. Equal mean occupation of black and white sites is also permitted. The black sites are labeled with index 1, the white sites with index 2.

On the lattice of Fig. 1 one can imagine subfigures, consisting in the simplest nontrivial case (Bethe-or quasi chemical approximation) of two nearest neighbour sites occupied in different ways. The trivial subfigure is simply a single lattice-site, either occupied with a particle or empty.

Figure 2 shows the different subfigures which can be built up by two nearest neighbour sites occupied in different ways. The meaning is: + an occupation with a particle — an occupation with a hole.

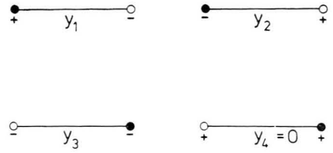

Fig. 2. Elementary subfigures on the lattice built up by two nearest neighbour lattice sites with their statistical weights: y_1, y_2, y_3, y_4.

For the subfigures in Fig. 2 it is also possible, to define occupation numbers with ensemble averages y_1, y_2, y_3, y_4.

Given an ensemble consisting of L lattices of the species of Fig. 1, each containing V lattice sites, one can ask, how many possible ways are there to occupy the lattices of this ensemble with particles in such a manner that in the statistical mean and, under the conditions described in the introduction, the ensemble averages of the occupation numbers $\langle\varepsilon\rangle(1) = \varrho_1$, $\langle\varepsilon\rangle(2) = \varrho_2$, y_1, y_2, y_3 are correctly reproduced.

Approximately this task is soluble. One may fill up at the same time the lattices of the ensemble row after row and count the number of possibilities of occupation. As sketched in Fig. 3, there are two different cases.

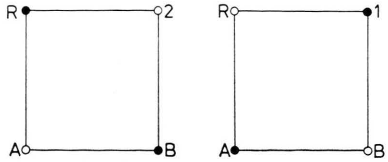

Fig. 3. Demonstration figures for the right statistical occupation of the two lattice sites 1 and 2.

In the one case site 1 is to be occupied in the correct ensemble average with the mean occupation number ϱ_1 under the premise that the sites R and B had been occupied with the correct mean occupation number ϱ_2. In a complete treatment it would be necessary to consider in addition the right mean occupation by the subfigures (R, 1) and (B, 1) with the ensemble averages $y_1 - y_4$. If only the correct mean occupation by subfigures (R, 1) is exactly considered, one gets:

$$g_{\mathrm{L}}^1 = \frac{(\varrho_2 L)!\,((1-\varrho_2)L)!}{(y_1 L)!\,(y_2 L)!\,(y_3 L)!}$$

possibilities for black sites 1.

The additive exact consideration of the mean occupation by subfigures (B, 1) with the right mean occupation numbers $y_1 - y_4$ is in general too difficult, so that an approximate treatment by a correction-factor

$$\Gamma_{\mathrm{L}}^1 = \frac{(\varrho_2 L)!\,((1-\varrho_2)L)!}{(y_1 L)!\,(y_2 L)!\,(y_3 L)!} \Bigg/ \frac{L!}{(\varrho_1 L)!\,((1-\varrho_1)L)!}$$

is a suitable way out.

The total number of possibilities of occupying sites 1 in an ensemble of L lattices under the conditions declared above is then:

$$G_L^1 = \frac{[(\varrho_2 L)!]^2\,[((1-\varrho_2)L)!]^2\,(\varrho_1 L)!\,((1-\varrho_1)L)!}{[(y_1 L)!\,(y_2 L)!\,(y_3 L)!]^2\,L!} \tag{5}$$

In the second case all is simply reversed. The number G_L^2 of possibilities for the occupation of sites 2 is obtained by replacing in formula (5) ϱ_2 by ϱ_1 and ϱ_1 by ϱ_2. Because one lattice of the L ensemble lattices has altogether V lattice sites, where $V/2$ black sites with index 1 and $V/2$ white sites with index 2 have to be occupied correctly, we have as a result

$$W = (G_L^1)^{V/2L} \cdot (G_L^2)^{V/2L} \tag{6}$$

different configurations on one lattice.

Approximating the sum $\sum\limits_{\varrho_1}\sum\limits_{\varrho_2}$ in (4) by its largest term, on account of (3), $W(\varrho_1, \varrho_2)$ may be connected approximately with the entropy S by the fundamental Boltzmann equation

$$S = k \ln[W(\varrho_1, \varrho_2)]\,. \tag{7}$$

The variables ϱ_1, ϱ_2, y_1, y_2, y_3 in G_L^1 and G_L^2 are not independent, but satisfy the following compatibility conditions:

$$\varrho_1 = y_1;\ \varrho_2 = y_2;\ 1 - \varrho_1 = y_2 + y_3; \tag{8}$$
$$(1 - \varrho_2) = y_1 + y_3;\ y_1 + y_2 + y_3 = 1\,.$$

The last equation for the y_i follows from the first equations.

A further very important condition is the hard-core condition

$$y_4 = 0 \tag{9}$$

which considers that simultaneous occupation of nearest neighbour lattice sites with particles is excluded. On account of (9) there is no y_4 in the formulas for G_L^1 and G_L^2. y_1, y_2 and y_3 in G_L^1 and G_L^2 can be expressed on account of (9) by the following functions:

$$y_1 = \varrho_1; \; y_2 = \varrho_2; \; y_3 = 1 - \varrho_1 - \varrho_2 \, . \tag{10}$$

Using now the Eqs. (5)—(10) and the Stirling-formula for great values of L, one gets as a result the following formula for the entropy of the lattice gas.

$$S = \frac{k\,V}{2} \{3(1-\varrho_1)\ln(1-\varrho_1) + 3(1-\varrho_2)\ln(1-\varrho_2) \\ - \varrho_1 \ln(\varrho_1) - \varrho_2 \ln(\varrho_2) - 4(1-\varrho_1-\varrho_2)\ln(1-\varrho_1-\varrho_2)\} \, . \tag{11}$$

The energy part of the grand partition function written in (4) in braces may now be written in the "mean-field" approximation:

$$\frac{1}{\beta} \ln \left\{ \frac{\sum\limits_{\varepsilon_1, \ldots, \varepsilon_V}' \exp\left[\beta \, \tfrac{1}{2} \sum\limits_{i,j=1}^{V} v_{ij}(\varepsilon_i, \varepsilon_j) + \beta\,\mu \sum\limits_{i=1}^{V} \varepsilon_i \right]}{W(\varrho_1, \varrho_2)} \right\} \approx$$

$$\approx \frac{V}{4} [v_1(\varrho_1)^2 + v_{12}\,\varrho_1\,\varrho_2 + v_2(\varrho_2)^2 + \tag{12}$$
$$+ v_{21}\,\varrho_2\,\varrho_1 + 2(\varrho_1+\varrho_2)\,\mu] \, .$$

Considering again the approximation of the sum $\sum\limits_{\varrho_1} \sum\limits_{\varrho_2}$ in (4) by its largest term on account of (3), (12) may be interpreted as $-(E - \mu N)$.

The zero-Fourier-components v_1, v_2, v_{12}, v_{21} in (12) are defined in the following way:

$$v_1 = \sum_{j=1}^{V/2}{}^{(1)} v_{ij} \, , \quad v_2 = \sum_{j=1}^{V/2}{}^{(2)} v_{ij} \, ,$$
$$v_{12} = \sum_{j=1}^{V/2}{}^{(2)} v_{ij} \, , \quad v_{21} = \sum_{j=1}^{V/2}{}^{(1)} v_{ij} \, , \tag{13}$$
$$v_1 + v_{12} = v_2 + v_{21} = v \, .$$

(1) and (2) in (13) are sum-indices which indicate that the sums are taken over the whole black- or white lattice, where pairs of indices (i, j) on the same site or nearest neighbour sites are not counted. For a lattice whose black and white sublattices are geometrically equivalent, as in our examples, because of symmetry the relations

$$v_1 = v_2; \quad v_{12} = v_{21} \tag{14}$$

are valid.

In later reflections and results the structure parameter $\bar{v}$, defined in (15), plays an important role.

$$\bar{v} = (1/v)\,(v_1 - v_{12}) \, . \tag{15}$$

Besides the parameter v from (13), which allows statements about the total strength of the soft interaction v_{ij}, the parameter $\bar{v}$ gives some more information about the geometrical structure of the interaction.

On account of the geometrical structure of v_{ij} particle occupations of the two sublattices black and white with different density (crystalline-structure) may be energetically prefered to a particle occupation with equal density on both sublattices (fluid structure). Such effects can thus considered. v_1, v_2, v_{12}, v_{21} can, of course easily, be expressed by v and $\bar{v}$.

The entropy of the linear lattice and the simple cubic lattice may be calculated now in quite the same way as the entropy of the plane square lattice in (11). It is only necessary in (11) to replace the number 3 by $z-1$ and the number 4 by z, where z is the coordination number of the lattice, to get a general formula of the entropy. Because the formula for $-(E - \mu N)$ (12) is independent of the lattice-type, one easily gets for the thermodynamic function $-pV = E - TS - \mu N$ of the lattice model the formula

$$p = \tfrac{1}{2} \{ \tfrac{1}{2} v_1(\varrho_1)^2 + \tfrac{1}{2} v_{12}\,\varrho_1\,\varrho_2 + \tfrac{1}{2} v_2(\varrho_2)^2 + \tfrac{1}{2} v_{21}\,\varrho_2\,\varrho_1 + (\varrho_1+\varrho_2)\,\mu \\ + 1/\beta\,[(z-1)(1-\varrho_1)\ln(1-\varrho_1) + (z-1)(1-\varrho_2)\ln(1-\varrho_2) - \varrho_1\ln(\varrho_1) - \varrho_2\ln(\varrho_2) \\ - z(1-\varrho_1-\varrho_2)\ln(1-\varrho_1-\varrho_2)]\} \, . \tag{16}$$

The distribution with the largest statistical weight, one gets by minimization of

$$-pV = E - TS - N$$

in Equation (16). The result is two coupled equations of state,

$$\frac{\partial p}{\partial \varrho_1} = \tfrac{1}{2}\left\{ v_1 \varrho_1 + v_{12}\,\varrho_2 + \mu - \frac{1}{\beta} \ln\left[\frac{(1-\varrho_1)^{z-1}\,\varrho_1}{(1-\varrho_1-\varrho_2)^z}\right]\right\} = 0\,, \tag{17}$$

$$\frac{\partial p}{\partial \varrho_2} = \tfrac{1}{2}\left\{ v_2 \varrho_2 + v_{21}\,\varrho_1 + \mu - - \frac{1}{\beta} \ln\left[\frac{(1-\varrho_2)^{z-1}\,\varrho_2}{(1-\varrho_1-\varrho_2)^z}\right]\right\} = 0 \tag{18}$$

for the two densities ϱ_1 and ϱ_2.

In the case of homogeneous occupation ($\varrho_1 \equiv \varrho_2 \equiv \varrho$) both Eqs. (17) and (18) degenerate into the single equation

$$\exp[\beta\,\mu] = \frac{\varrho\,(1-\varrho)^{z-1}}{(1-2\,\varrho)^z} \exp[-\beta\, v\, \varrho]\,. \tag{19}$$

The solution $\varrho_1(\mu, T) \equiv \varrho_2(\mu, T)$ is indeed possible, as is shown by a later general treatment of (17) and (18).

Combining (16) for $\varrho_1 = \varrho_2$ with (19) the equation of state for the fluid phases follows:

$$p = \frac{v}{2}\left[-\varrho^2 + \frac{1}{\beta v} \ln\left[\frac{(1-\varrho)^{2(z-1)}}{(1-2\,\varrho)^z}\right]\right]. \tag{20}$$

Between the mean density $\varrho = (\varrho_1 + \varrho_2)/2$ and the pressure p there exists through (16), (17) and (18) the important general relation

$$\mathrm{d}p/\mathrm{d}\mu = \tfrac{1}{2}\,(\varrho_1 + \varrho_2) = \varrho \tag{21}$$

by which p may be directly calculated from $\varrho(\mu)$ without knowledge of $\varrho_1(\mu)$ and $\varrho_2(\mu)$, if p is known for a single arbitrary value of ϱ.

3. Solution of the Equations for the Thermodynamic State-Variables by Separation and Subsequent Treatment by Graphic Methods

The equations of state (17), (18) may be easily transformed:

$$\begin{aligned}(1-\varrho_1)^{z-1}\,\varrho_1 \exp[\beta\,(v_1 - v_{12})\,(1-\varrho_1)] \\ = (1-\varrho_2)^{z-1}\,\varrho_2 \exp[\beta\,(v_2 - v_{21})\,(1-\varrho_2)] \\ = (1-2\,\varrho)^z \exp[-\beta\, v_{12}\,(1-2\,\varrho)] \exp[\beta\,(v_1+\mu)]\,.\end{aligned} \tag{22}$$

Equation (22) splits into the three equations

$$\lambda = (1-\varrho_1)^{z-1}\,\varrho_1 \exp[\beta\, v\, \bar{v}\,(1-\varrho_1)]\,, \tag{23}$$

$$\lambda = (1-\varrho_2)^{z-1}\,\varrho_2 \exp[\beta\, v\, \bar{v}\,(1-\varrho_2)\,, \tag{24}$$

$$\lambda = (1-2\,\varrho)^z \exp[-\beta\, v_{12}\,(1-2\,\varrho)] \exp[\beta\,(v_1+\mu)], \tag{25}$$

with λ as a separation parameter, where (14) and (15) have also been used.

A graphical treatment of the system (23), (24) and (25) is now possible, as it is demonstrated in Figure 4.

The functions $\lambda(\varrho_1)$ and $\lambda(\varrho_2)$ are, on account of (23) and (24), identical (continuous line in Fig. 4). Nevertheless, the reverse function $\varrho_{\mathrm{gl}}(\lambda)$ is ambiguous. One has two branches with a branching-point P.

By the aid of $\varrho_1(\lambda) + \varrho_2(\lambda) = 2\,\varrho_{\mathrm{s}}(\lambda)$, ($\varrho_1 > \varrho_2$) one can construct the dashed $\varrho_{\mathrm{s}}(\lambda)$-line in Figure 4.

The dotted line and the line which is composed of dots and dashes in Fig. 4 correspond to the function $\lambda_\mu(\varrho)$ of Eq. (25) and are adjoined to the two cases $v_{12} > 0$, $v_{12} < 0$.

These lines have points of intersection with the continuous $\varrho_{\mathrm{gl}}(\lambda)$-line and the dashed $\varrho_{\mathrm{s}}(\lambda)$-line. The ($\varrho$, λ)-coordinates of these points of intersection are dependent on β, μ and v, $\bar{v}$. The points of intersection on the continuous $\varrho_{\mathrm{gl}}(\lambda)$-line belong to the fluid phases with homogeneous particle occupation. The points of intersection on the dashed $\varrho_{\mathrm{s}}(\lambda)$-line belong to the solid phase with periodic particle occupation. The indices s, g, l stand here and in the whole publication as abbreviations for solid, gaseous and liquid respectively.

In the case $v\bar{v} < 0$ there is, since $\varrho(P) > 0{,}5$ for very deep temperatures, non branching-point P in the physically interesting area. Only for increasing temperatures, more exactly when $\beta v \bar{v} > 2\,(2-z)$, a real branching-point P exists and if $\beta \to 0$, the lines for $v\bar{v} < 0$ coalesce, the lines for $v\bar{v} > 0$.

As a result of the graphical construction sketched above, one gets the ϱ (μ)-curves drawn in Fig. 5 for the case $v > 0$.

If the temperature increases, the points $\mathrm{P_g}$ and $\mathrm{P_l}$ in Fig. 5 melt into one another when the critical point of condensation is reached and they vanish for higher temperatures.

Therefore the critical point of condensation is defined by the vanishing of the first and second

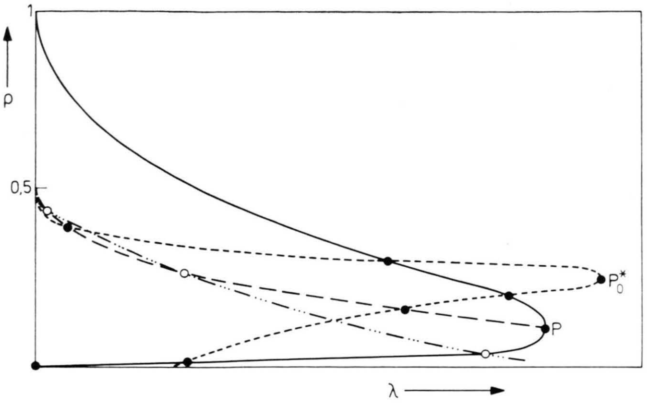

Fig. 4. Construction-figure for the graphical determination of the $\varrho(\mu)$-isotherms of the lattice gas in the case $v\bar{v} > 0$.

derivative of the function $\mu(\varrho)$ in (19). This leads to the two equations

$$(1 - 2\varrho_{\mathrm{cgl}})^3 - \frac{3z}{2(z-2)}(1 - 2\varrho_{\mathrm{cgl}})^2 + \frac{z}{2(z-2)} = 0\,. \tag{26}$$

$$\beta_{\mathrm{cgl}}\frac{v}{2} = \frac{z}{1 - 2\varrho_{\mathrm{cgl}}} + \frac{1}{2\varrho_{\mathrm{cgl}}} - \frac{z-1}{2(1-\varrho_{\mathrm{cgl}})} \tag{27}$$

for the critical density and the critical temperature of the lattice gas.

As a further result one gets at once the whole critical data of the lattice gas, which are presented in Table 1.

Table 1. Critical data of the lattice gas model for the transition gas-liquid.

	ϱ_{cgl}	$\beta_{\mathrm{cgl}}\,v$	μ_{cgl}	p_{cgl}
$z = 2$	0.21	10.5	$-0.27\,v$	$0.006\,v$
$z = 4$	0.175	14.4	$-0.19\,v$	$0.005\,v$
$z = 6$	0.15	16	$-0.18\,v$	$0.004\,v$

If the temperature increases above the critical point of condensation a point is reached, where the branching-point P and the extremal-point P_s of the function $\mu(\varrho)$ in Fig. 5 melt into one another. This is the critical point of the phase transition fluid-solid.

The critical point of the phase transition fluid-solid is therefore defined by the two equations

$$\beta_{\mathrm{cgs}}\,v = \frac{1}{\bar{v}}\left[\frac{1}{\varrho_{\mathrm{cgs}}} - \frac{z-1}{1-\varrho_{\mathrm{cgs}}}\right], \tag{28}$$

$$\begin{aligned}\bar{v} = {} & (1 - 2\varrho_{\mathrm{cgs}})\,[(2-z) + z(1 - 2\varrho_{\mathrm{cgs}})]\\ & [(z-1)\,(\varrho_{\mathrm{cgs}})^3 - (1-\varrho_{\mathrm{cgs}})^3]/\{4z\,\varrho_{\mathrm{cgs}}(1-\varrho_{\mathrm{cgs}})\,\cdot\\ & [(z-1)\cdot(\varrho_{\mathrm{cgs}})^3 - (1-\varrho_{\mathrm{cgs}})^3] + (1 - 2\varrho_{\mathrm{cgs}})\,\cdot\\ & \cdot[((2-z) + z(1 - 2\varrho_{\mathrm{cgs}}))\cdot((z-1)\,(\varrho_{\mathrm{cgs}})^3\\ & - (1-\varrho_{\mathrm{cgs}})^3) + 3\,((z-1)\,(\varrho_{\mathrm{cgs}})^2 + (1-\varrho_{\mathrm{cgs}})^2)^2]\}\,.\end{aligned} \tag{29}$$

By the aid of the Eqs. (19), (20) all other critical data of the lattice gas are easily derived. They depend essentially on the interaction-structure-parameter $\bar{v}$ and they are drawn for the lattice gas as dashed lines in the phase diagrams Figs. 7 and 8.

At still higher temperatures no points P_g, P_l, P_s in Fig. 5 will exist. The functions $\varrho(\mu)$ and $p(\mu)$ then take a monotonous ascending course.

The branching-point P exists up to arbitrarily high temperatures. There are the limits: $\beta v \to 0$, $\varrho(\mathrm{P}) \to 1/z$ and $\mu(\mathrm{P}) \to \infty$ for all cases.

On account of (21), one easily interprets $\varrho(\mu)$ as the slope of the function $p(\mu)$ and constructs the $p(\mu)$-curves, sketched in Figure 6. The $p(\mu)$-curves in Fig. 6 correspond to the $\varrho(\mu)$-curves of Figure 5. The $p(\mu)$-curves are extremely important, because one can recognize by them, in which phase the lattice gas will be found: The stable thermodynamic state in equilibrium is defined by the lowest $-pV$.

The continuous line in Fig. 6, which describes the fluid phase in the case $v > 0$, has the two asymptotes

$$p \to 0 \text{ and } p \to \tfrac{1}{2}\left(\frac{v}{4} - \frac{z-2}{\beta}\ln 2 + \mu\right)$$

for $\mu \to -\infty$ and $\mu \to +\infty$ respectively.

The dashed lines in Fig. 6, which correspond to the solid phase, have the asymptote

$$p = \tfrac{1}{2}\left(\frac{v}{4} + \frac{v\bar{v}}{4} + \mu\right) \text{if } \mu \to \infty.$$

From Fig. 6 it is evident that in the case $v\bar{v} > 0$ there exist two transition points $\mathrm{Ph}_{\mathrm{lg}}$ and $\mathrm{Ph}_{\mathrm{sl}}$ which are connected to the condensation and the freezing of the lattice gas. But the condensation point, following the $p(\mu)$-curve from negative to positive values of μ will not be reached, because the gas phase changes already at the freezing point $\mathrm{Ph}_{\mathrm{sl}}$ into the crystalline phase.

The crystalline phase remains stable for all values of μ with $\mu > \mu_{\mathrm{ls}}$, because in this domain this phase has a lower $-pV$, and thus a greater statistical weight than the fluid phase.

In the case $v\bar{v} < 0$ for low temperatures there is only the condensation point $\mathrm{Ph}_{\mathrm{lg}}$.

The fluid phase has in the whole μ-domain a lower $-pV$ than the solid phase and is stable there on this account.

Only when the domain
$\beta v \bar{v} \gtreqless \beta_\infty v \bar{v} = -4(z-2)\ln 2$
is reached, the second transition point $\mathrm{Ph}_{\mathrm{ls}}$ arises where $\mu_{\mathrm{ls}} > \mu_{\mathrm{lg}}$.

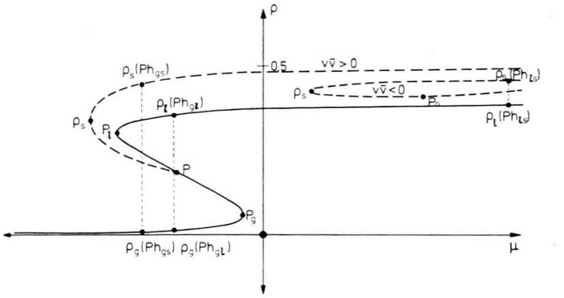

Fig. 5. $\varrho(\mu)$-isotherms of the lattice gas with attractive total interaction ($v > 0$) at low temperatures. ——— fluid phases; ------- solid phases for $v\bar{v} \gtreqless 0$.

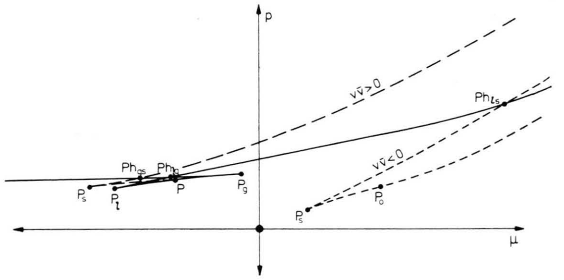

Fig. 6. $p(\mu)$-isotherms of the lattice gas with attractive total interaction at low temperatures. ——— fluid phases; ------- solid phases for $v\bar{v} \gtreqless 0$.

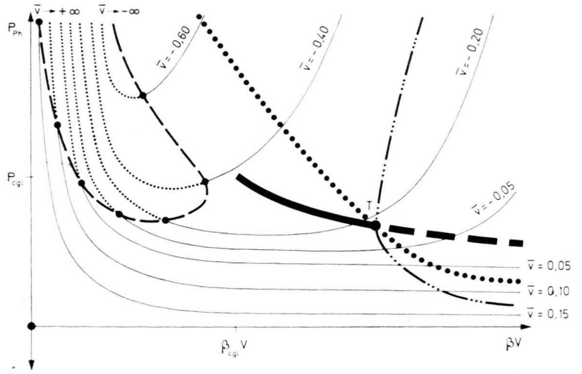

Fig. 7. The pressure p_{Ph} of the lattice gas on the curves of coexistence as a function of βv, for attractive total particle interaction ($v > 0$), for the two- and three dimensional lattice.

Following the $p(\mu)$-curve from negative to positive values of μ, only on branches with lowest $-pV$ first a condensation to a liquid occurs at the point $\mathrm{Ph}_{\mathrm{lg}}$. At still greater values of μ freezing, will take place at the point $\mathrm{Ph}_{\mathrm{ls}}$. The solid phase remains stable for μ-values greater than that of $\mathrm{Ph}_{\mathrm{ls}}$.

For increasing temperatures the transition point $\mathrm{Ph}_{\mathrm{lg}}$ vanishes at the critical point of the fluid phases.

The transition point $\mathrm{Ph}_{\mathrm{ls}}$ exists for all temperatures and coincides for temperatures above the critical point of the solid-fluid phase transition with the branching-point P.

Therefore always a transition from the fluid phase to the solid phase exists.

If the "smooth" total particle interaction is repulsive ($v < 0$) the $\varrho(\mu)$ and $p(\mu)$-curves of the homogeneous distribution take a similar course as the continuous lines in Figs 5 and 6, but ascending monotonously and without the extremal points P_l and P_g.

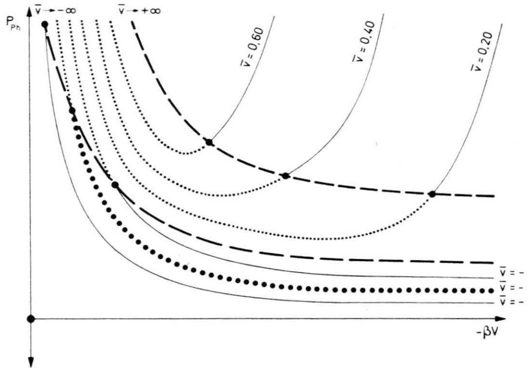

Fig. 8. The pressure p_{Ph} of the lattice gas on the curves of coexistence as a function of $-\beta v$ for repulsive total particle interaction ($v < 0$), for the two- and three dimensional lattice.

For very low temperatures the function $\varrho(\mu)$ of the homogeneous distribution changes into the function $\varrho = 0$ if $\mu < -\frac{1}{4}v$ and $\varrho = \frac{1}{2}$ if $\mu > -\frac{1}{4}v$, where at the point $\mu = -\frac{1}{4}v$ a threshold is built up. The function $p(\mu)$ is then practically represented by the two asymptotes.

The functions $\varrho(\mu)$ and $p(\mu)$ of the periodical occupation depend essentially on $v\bar{v}$. They therefore show for $v < 0$ the same course as the dashed lines in Figures 5 and 6. The only difference is, that in the interval $-2 < \bar{v} < 0$ no extremal point P_s exists. On the $p(\mu)$-curve only the transition point $\mathrm{Ph}_{\mathrm{ls}}$ is present.

If $v\bar{v} > 0$, Ph_{1s} exists again down to lowest temperatures. If $v\bar{v} < 0$, Ph_{1s} exists only above the temperature $\beta_\infty v\bar{v}$. For lower temperatures there exists again only the fluid phase.

At the critical point of the fluid-solid transition P again coincides with Ph_{1s}.

In the case $v < 0$ also, for all values of μ with $\mu > \mu_{1s}$ the solid phase, because of its lower $-pV$ compared to the fluid phase, is found in the stable state.

If $-2 < \bar{v} < 0$, $v < 0$, Ph_{1s} coincides for all temperatures with the branching point P. Sublimation then occurs without discontinuity.

While the discontinuous increasing of the density in the fluid phase can not occur for temperatures above the critical point, freezing takes place in principle at all temperatures. Above its critical point freezing of course is no longer coupled with a discontinuity in density.

Below the critical points all phase changes are connected with discontinuities in the density of the lattice gas.

The densities of the lattice gas on the curves of coexistence are easily available from Fig. 5, after one has gained $\mu_{\mathrm{Ph}}(\beta)$ and $p_{\mathrm{Ph}}(\beta)$ at the phase transition points from the $p(\mu)$-diagram (Figure 6).

A complete pressure-temperature ($p - \beta v$) phase diagram of the curves of coexistence for $v > 0$ is given in Figure 7. The same phase diagram is drawn for $v < 0$ in Figure 8.

One recognizes in Fig. 7 and Fig. 8, that the right semi-planes of the $p_{\mathrm{Ph}} - \beta v$ coordinate planes are covered with nets of thin lines, which represent the fluid-solid transition curves. These phase transition curves, which depend on the interaction-structure-parameter $\bar{v}$, lead, at temperatures which are higher than the critical temperature of condensation, to the (dashed) critical curves of the transition fluid-solid.[41]

In Fig. 7 for the case $v > 0$ the $p_{\mathrm{Ph}} - \beta v$ condensation curve is painted as a heavy continuous and heavy dashed line. There is qualitative agreement of this curve with experiment.

The thin curves of coexistence in Fig. 7 and Fig. 8 of the fluid-solid transitions depending on $\bar{v}$, do not uniquely define the real $p_{\mathrm{Ph}} - \beta v$ fluid-solid transition curves of the systems. Only in assuming a functional dependence $\bar{v}(\beta v)$ of the interaction-structure-parameter $\bar{v}$, is one able to define uniquely and entirely the fluid-solid transition curve in optimal semiempirical adaptation to the experimental results.

In Fig. 7 the curve of coexistence for the fluid-solid transition, corresponding to phase diagrams of inert gases is shown with a dotted line.

The fluid-solid transition curve intersects the curve of condensation in a triple point. At temperatures below the triple point, there exists only the transition curve gaseous-solid, because $\bar{v} > 0$; therefore the curve of condensation had been drawn there with a heavy dashed line.

For a solid-fluid transition, as is observed for the system water-ice, it is also possible to insert into the net of fluid-solid transition curves a corresponding curve of coexistence. Such a transition curve is sketched in Fig. 7 as a medium heavy line composed dotts and dashes.

The transition curve of the fluid-solid transition constructed in Fig. 7 by semiempirical adaptation recourses that for the temperature dependence of the interaction-structure-parameter $\bar{v}$ a function must be taken into account similar to that sketched in Figure 9.

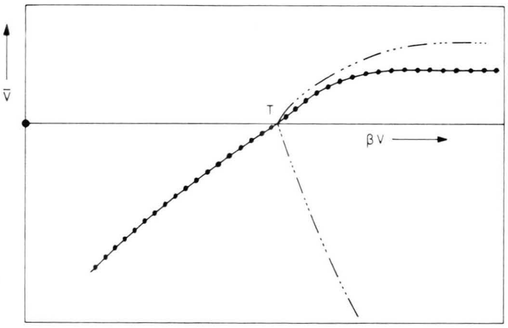

Fig. 9. The interaction-structure-parameter $\bar{v}$ as a function of βv for the two — and three dimensional lattice (continuously dotted and alternately dotted lines correspond to analogous curves in Figure 7).

From physical reasoning one has to suppose that $\bar{v}$ for higher and higher temperatures tends towards a finite limit.

By that, the critical point of sublimation is uniquely defined. It will always be situated at very high temperatures and very high pressures. This is a domain, where measurements are up to-day very hard to perform.

$\bar{v}$ of a gas with smooth, repulsive total interaction (one could imagine a strong ionized gas as an example) apparently is not much to be changed with temperature, if one wishes to insert a real curve of coexistence of the fluid-solid transition into the net of lines in Figure 8. The dotted painted fluid-solid transition curve in Fig. 8 is therefore a curve with a fixed negative value of $\bar{v}$, where $\bar{v} < -2$.

Having constructed the $p(\beta v)$-phase diagrams for the lattice gas by assuming a suitable function $\bar{v}(\beta v)$, the complete state diagram can easily be constructed. In Fig. 10 for a gas with an attractive mean soft interaction part ($v > 0$) the $p - \varrho$ isotherms are plotted. The curve of coexistence for the transition fluid → solid corresponds to a semi-empirical $\bar{v}(\beta v)$-function, drawn in Figure 9. Above its critical point (p_{cgs}, ϱ_{cgs}) this transition curve degenerates into a single line, indicating that no discontinuity in density will take place.

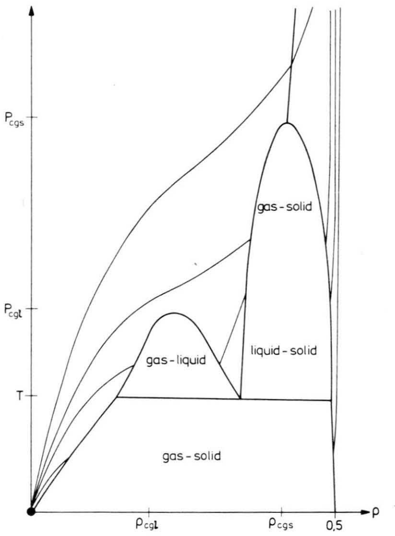

Fig. 10. The pressure-density state diagram with curves of coexistence for attractive total particle interaction ($v > 0$) for the two- and three dimensional lattice.

Like the Ising lattices gas is related to a classical Ising magnet, the lattice gas model of this paper is related to a corresponding classical magnet which has one ferrimagnetic and two ferromagnetic stable phases with accompanying phase transitions. The peculiarity of this magnetic model is that the magnetism can occur *only in one direction*, contrary to the classical Ising magnet.

The necessity of constructing a function $\bar{v}(\beta v)$ (Fig. 9) by semi-empirical adaption to agree with experimental results is a weakness of the theory, which perhaps may be removed by a better statistical consideration of the hard core correllation.

Contrary to the transition fluid-solid the condensation depends largely neither on the detailed structure of the interaction nor on the dimensionality of the lattice, at least in Kikuchi-approximation.

The theory developed in this publication states only that besides a condensation, a crystallization and a sublimation may also occur. To the question, into which types of lattices for a definite particle interaction the real gas will crystallize, no answer is given by the theory.

The author thanks Prof. Dr. Franz Rys, Institut für Theoretische Physik der FU Berlin, for helpful discussions.

[1] T. D. Lee and C. N. Yang, Phys. Rev. **87**, 410 [1952].

[2] H. S. Green and C. A. Hurst, Order — Disorder Phenomena, Interscience Publishers, New York 1964.

[3] A. Münster, Statistische Thermodynamik, Springer-Verlag, Heidelberg 1956.

[4] T. H. Berlin and M. Kac, Phys. Rev. **86**, 821 [1952].

[5] M. Kac and J. C. Ward, Phys. Rev. **88**, 1332 [1952].

[6] R. Brout, Phys. Rev. **122**, 469 [1961].

[7] R. Kikuchi, Phys. Rev. **81**, 988 [1951].

[8] C. Domb and M. F. Sykes, Adv. in Phys. **9**, 245 [1960].

[9] F. H. Stillinger, Jr., Phys. Rev. **135**, 1645 [1964].

[10] R. Kikuchi and S. G. Brush, J. Chem. Phys. **47**, 195 [1967].

[11] C. A. Hurst, J. Math. Phys. **7**, 305 [1966].

[12] A. J. F. Siegert and D. J. Vezzetti, J. Math. Phys. **9**, 2173 [1968].

[13] T. Tsang, Physica **42**, 1 [1969].

[14] E. Helfand, Phys. Rev. **180**, 600 [1969].

[15] F. Schwabl, Ann. Physics **54**, 1 [1969].

[16] H. N. V. Temperley, Proc. Phys. Soc. London A **67**, 233 [1954].

[17] H. N. V. Temperley, Proc. Phys. Soc. London B **70**, 536 [1957].

[18] H. N. V. Temperley, Proc. Phys. Soc. London B **77**, 630 [1961].

[19] D. M. Burley, Proc. Phys. Soc. London B **85**, 1173 [1965].

[20] D. S. Gaunt and M. E. Fisher, J. Chem. Phys. **43**, 2840 [1965].

[21] F. H. Ree and D. A. Chesnut, J. Chem. Phys. **45**, 3983 [1966].

[22] J. L. Lebowitz and J. K. Percus, Phys. Rev. **144**, 251 [1966].

[23] P. Hutchinson, Mol. Phys. **13**, 495 [1967].

[24] L. K. Runnels, J. Math. Phys. **8**, 2081 [1967].

[25] W. G. Hoover and F. H. Ree, J. Chem. Phys. **49**, 3609 [1968].

[26] J. Orban and A. Bellemans, J. Chem. Phys. **49**, 363 [1968].

[27] J. Orban, J. van Craen, and A. Bellemans, J. Chem. Phys. **49**, 1778 [1968].

[28] C. Fan and F. Y. Wu, Phys. Rev. **179**, 560 [1969].

[29] G. Gallavotti and S. Miracle-Sole, J. Math. Phys. **11**, 147 [1970].

[30] L. K. Runnels, J. Math. Phys. **11**, 842 [1970].

[31] R. J. Baxter, J. Math. Phys. **11**, 3116 [1970].

[32] N. F. Carnahan and K. E. Starling, J. Chem. Phys. **53**, 600 [1970].

[33] W. G. Hoover, M. Ross, K. W. Johnson, D. Henderson, J. A. Barker, and B. C. Brown, J. Chem. Phys. **52**, 4931 [1970].

[34] A. L. Beyerlein, W. G. Rudd, Z. W. Salsburg, and M. Buynoski, J. Chem. Phys. **53**, 1532 [1970].

[35] I. Syozi, Progr. Theoret. Phys. **39**, 1367 [1968].

[36] S. Miyazima and I. Syozi, Progr. Theoret. Phys. **40**, 185 [1968].

[37] H. Nakano, Progr. Theoret. Phys. **40**, 231 [1968].

[38] I. Syozi and H. Nakano, Progr. Theoret. Phys. **40**, 237 [1968].

[39] H. Nakano and K. Yamada, Progr. Theoret. Phys. **41** 350 [1969].

[40] K. Yamada, Progr. Theoret. Phys. **42**, 1106 [1969].

[41] The dotted parts of the thin fluid-solid transition curves in Fig. 7 and Fig. 8 represent the supercritical continuous order-disorder transitions. The fluid-solid transition curves in Fig. 8 with $-2<\bar{v}<0$ are not drawn for graphical reasons. They must be imagined as dotted lines, lying between the curves with $\bar{v}<-2$ and the curves with $\bar{v}>0$, representing there continuous order-disorder transitions in the whole region of temperature.